Electrochemistry and Electrogenerated Chemiluminescence of Quinoxaline Derivatives

Anahita Izadyar,‡ Khalid M. Omer,‡ Yunqi Liu,† Shiyan Chen,† Xinjun Xu,† and Allen J. Bard*,‡

Center for Electrochemistry, The University of Texas at Austin, Chemistry and Biochemistry Department, Austin, Texas 78712, and National Laboratory for Molecular Sciences, Institute of Chemistry, Chinese Academy of Sciences, Beijing 100190, P. R. China

Received: August 12, 2008; Revised Manuscript Received: October 17, 2008

We report the electrochemistry, spectroscopy, and electrogenerated chemiluminescence (ECL) of donor−acceptor compounds containing a quinoxaline derivative as the central core coupled with fluorene (**CFPQ**, **CFPP**, and **MFPQ**) and triphenylamine moieties (**MAPQ**). Cyclic voltammetry of all four derivatives show reversible reduction waves (assigned to the formation of the radical anion) localized in the quinoxaline moiety (the acceptor group), whereas oxidation waves show behavior that depends upon the nature of the donor group. With a pair of strong donor groups, triphenylamine, (**MAPQ**), exhibits a two electron oxidation wave due to the two noninteracting donor moieties. The fluorene derivatives (**CFPQ**, **CFPP**, and **MFPQ**) show less reversible oxidation waves at scan rates of 100 mV/s, but **CFPP** and **CFPQ** become reversible at higher scan rates. In their absorbance and emission spectra, all of the compounds, except **MFPQ**, exhibit large Stokes shifts, which are related to the rearrangement of the excited-state and also to solvent effects. ECL was observed for **MAPQ**, **CFPQ**, and **CFPP** in MeCN/benzene solutions that generally agree with the photoluminescence spectra, suggesting that the energy of annihilation is sufficient to form singlet excited states (the S-route). The ECL of **MAPQ** was strong enough to be seen with the naked eye. **MFPQ** did not produce ECL, probably because of the instability of the radical cation.

Introduction

We present in this report electrochemistry and electrogenerated chemiluminescence (ECL) of a series of donor−acceptor compounds containing a quinoxaline (Q) derivative[1] whose structures are shown in Scheme 1. We represent these as X−Q−X, where Q represents the quinoxaline center and X the substitutents (triphenylamine or fluorene). These π-conjugated donor−acceptor (D−π−A) materials have unique optical and electrical properties, which have potential applications in many fields such as light-emitting diodes (OLEDs),[2,3] field-effect transistors (FETs),[4] nonlinear optics (NLO),[5] and photovoltaic devices.[6] These compounds have high thermal stability and show bright light-emission varying from blue to red due to different strengths of the donor and acceptor. Such π-conjugated donor−acceptor (D−A) compounds have been used previously in electrochemical and ECL experiments to probe the stability of the radical ions formed on redox reactions as well as structural effects on the electrochemical behavior.[3,7,8]

ECL is now a well-established field[9,10] and can even be used down to the single nanoparticle level.[11] ECL involves the formation of electronically excited states by electron transfer reactions between radical ions (or other highly oxidized and reduced species). The oxidized and reduced species are generated at an electrode by alternating pulses of the electrode potential. This process has been extensively investigated and used in studying reactions. This simplest ECL process (the radical ion annihilation reaction sequence) can be represented as

$$\mathrm{R} - \mathrm{e}^- \rightarrow \mathrm{R}^{+\bullet} \quad \text{(oxidation at electrode)} \tag{1}$$

$$\mathrm{R} + \mathrm{e}^- \rightarrow \mathrm{R}^{-\bullet} \quad \text{(reduction at electrode)} \tag{2}$$

$$\mathrm{R}^{+\bullet} + \mathrm{R}^{-\bullet} \rightarrow {}^1R^* + R \quad \text{(singlet excited state formation)} \tag{3}$$

$${}^1R^* \rightarrow R + h\nu \quad \text{(light emission)} \tag{4}$$

Many ECL reactions of this type have been investigated and their mechanisms are well understood.

If the energy provided by the ion radicals is not sufficient to populate the singlet state, the triplet state can be populated (eq 5), followed by triplet−triplet annihilation to generate the singlet state (eq 6). This is called the T-route or an "energy deficient" system.

$$R^{+\bullet} + R^{-\bullet} \rightarrow {}^3R^* + R \quad \text{(triplet excited state formation)} \tag{5}$$

$${}^3R^* + {}^3R^* \rightarrow {}^1R^* + R \quad \text{(triplet triplet annihilation)} \tag{6}$$

The search for new, highly efficient, and stable organic and inorganic ECL emitters has been a continuous theme in ECL (e.g., as emitting labels in analytical applications). Successful ECL emitters must be capable of generating radical cations and anions that are stable even after prolonged electrochemical cycling and ECL production.[12,13] ECL is also useful in probing how the structure of the radical ions of R, or other species, can affect the electron transfer reaction that produces the excited state.

We show in this paper how ECL measurements can be used to gain thermodynamic information about **MAPQ**, **CFPQ**, and **CFPP**. In the ECL experiments, excited states are generally

* To whom correspondence should be addressed. E-mail: ajbard@mail.utexas.edu.
‡ The University of Texas at Austin.
† Chinese Academy of Sciences.

10.1021/jp807202d CCC: $40.75 © 2008 American Chemical Society
Published on Web 11/21/2008

SCHEME 1: Chemical Structures of Compounds Used, MAPQ, CFPQ, CFPP, and MFPQ[a]

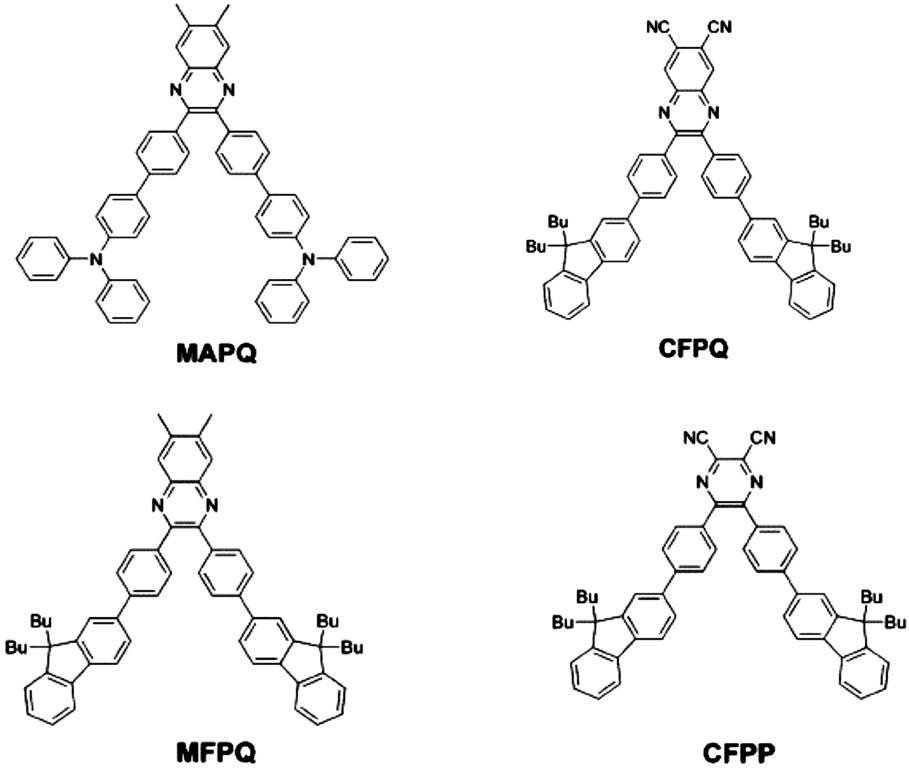

[a] 6,7-Dimethyl-2,3-di-(4′-diphenylamino-biphenyl-4-yl)-quinoxaline (**MAPQ**); 6,7-dimethyl-2,3-di-[4-(9,9-dibutyl-9 *H*-fluoren-2-yl)-phenyl]-quinoxaline (**MFPQ**); 2,3-dicyano-5,6-di-[4-(9,9-dibutyl-9 *H*-fluoren-2-yl)-phenyl]-pyrazine (**CFPP**); 6,7-dicyano-2,3-di-[4-(9,9-dibutyl-9 *H*-fluoren-2-yl)-phenyl]-quinoxaline (**CFPQ**).

produced by electron transfer between oxidized and reduced species generated at an electrode by alternating potential steps or sweeps.

Experimental Section

Chemicals. The compounds were synthesized as described previously.[1] The 6,7-dimethyl-2,3-di-(4′-diphenylamino-biphenyl-4-yl)-quinoxaline (**MAPQ**) was synthesized as a pale yellow solid in 94% yield; 6,7-dicyano-2,3-di-[4-(9,9-dibutyl-9 *H*-fluoren-2-yl)-phenyl]-quinoxaline (**CFPQ**) was synthesized as a yellow solid in 88% yield; 6,7-dimethyl-2,3-di-[4-(9,9-dibutyl-9 *H*-fluoren-2-yl)-phenyl]-quinoxaline (**MFPQ**) was synthesized as a pale yellow solid in 92% yield; 2,3-dicyano-5,6-di-[4-(9,9-dibutyl-9 *H*-fluoren-2-yl)-phenyl] (**CFPP**) was synthesized in 95% yield.[1] Anhydrous acetonitrile (MeCN, 99.8% in a sure-sealed bottle) and anhydrous benzene (Bz, 99.9% in a sure-sealed bottle) were obtained from Aldrich. Tetra-*n*-butylammonium perchlorate (TBAP) and tetra-*n*-butylammonium hexafluorophosphate ($TBAPF_6$) were obtained from Fluka and transferred directly into a He atmosphere glovebox. All solutions were prepared in a glovebox in an airtight cell for measurements completed outside the box.

Apparatus and Instrumentation. Electrochemical methods such as multipotential step and cyclic voltammetry (CV) were performed with a conventional three-electrode cell linked to a CH Instruments electrochemical workstation model 660 (Austin, TX). The working electrode, in most cases, consisted of an inlaid Pt disk (1.0−2.0 mm in diameter) that was polished on a felt pad with 0.3 μm alumina, followed by 0.05 μm alumina (Buehler, Ltd., Lake Bluff, IL), sonicated in water and absolute ethanol for 5 min, and dried in a oven at 100 °C. A Pt wire served as a counter electrode and a Ag wire as a quasi reference electrode (QRE). All potentials were calibrated against SCE by the addition of ferrocene (Fc) as an internal standard, taking $E^{\circ}_{Fc/Fc+} = 0.424$ V vs SCE.[14] The uncompensated resistance and double layer capacitance were obtained from a potential step experment in the potential region where no faradaic process occurred. Emission spectra were obtained with a charge coupled device (CCD) camera (Princeton Instruments, SPEC-10) that was cooled to −100 °C. The CCD camera and grating system were calibrated with a mercury lamp prior to each measurement. The ECL transients were measured with a photomultiplier tube (PMT, Hamamatsu R4220p) installed under the electrochemical cell. A voltage of −750 V was supplied to the PMT with a high-voltage power supply series 225 (Bertan High Voltage Corp., Hicksville, NY). All fluorescence spectra were recorded on a Fluorolog-3 spectrofluorimeter (ISA-Jobin Yvon Horiba, Edison, NJ). UV−vis spectra were recorded on a Milton Roy Spectronic 3000 array spectrophotometer. To generate ECL via ion annihilation, the working electrode potential was pulsed between the first oxidation and reduction peak potentials with a pulse width of 0.1 s. Digital simulations of cyclic voltammograms were performed with Digisim Software package 3.0 (Bioanalytical Systems), to investigate the mechanisms of the electrochemical processes.

Results and Discussion

Electrochemistry. Cyclic voltammograms of the compounds are shown in Figure 1, using either MeCN or a MeCN/Bz mixture as solvent; the latter was useful to increase the solubility to convenient levels. As shown in Figure 1 (and in the Supporting Information, Figure S1), the CV of **MAPQ** in MeCN:Bz (1:1) at a scan rate, v, of 100 mV/s showed a reversible oxidation wave with a half-wave potential $E_{1/2} = 1.26$

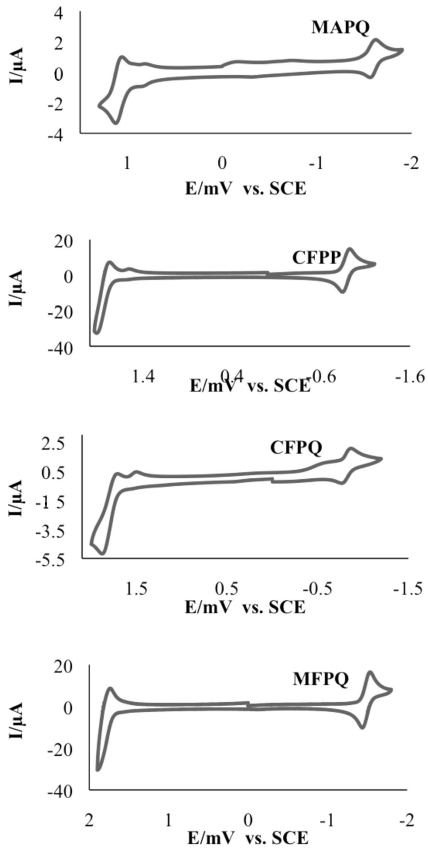

Figure 1. Cyclic voltammograms of 1 mM **MAPQ**, in benzene/acetonitrile (1:2 by volume) with 0.1 M TBAP as the supporting electrolyte, and in benzene/acetonitrile (1:1) with 0.1 M $TBAPF_6$ for 1 mM **CFPQ**, **CFPP**, and **MFPQ**. Scan rate at 0.1 V/s.

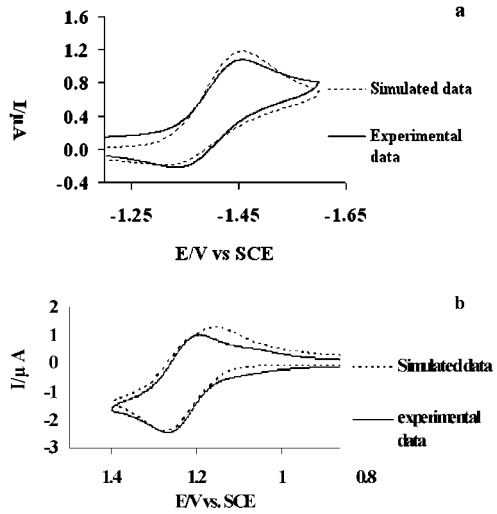

Figure 2. Comparison of the experimental and simulated data of 1 mM **MAPQ** (at $v = 50$ mV/s) there is a better fit if one adds a slow reaction of the radical anion following reduction of **MAPQ**, an EC mechanism (a). For the oxidation of **MAPQ** the simulation shows an EE scheme (b).

V vs SCE. The ease of oxidation can be attributed to the strong donor ability of the triphenylamine group. The negative scan shows a reversible reduction wave at $E_{1/2} = -1.72$ V. We assign the reduction of **MAPQ** to the quinoxaline group, which serves in all of these compounds as the electron acceptor. The oxidation peak current, $i_p^{oxd} = -25.2\ \mu$A, which is about twice that of the reduction peak current $i_p^{red} = 12.3\ \mu$A, with both reduction and oxidation waves reversible ($i_{pr}/i_{pf} \sim 1$ even at $v = 50$ mV/s). Thus the oxidation involves a two-electron transfer process (compared to the one electron reduction wave), suggesting that there is little interaction between the two triphenylamine groups through the quinoxaline group. The good chemical reversibility found in CV indicates high stability of both anion radical and dication moieties. We thus represent the electrode reactions as:

$$\text{reduction} \quad X{-}Q{-}X + e^- \rightarrow X{-}Q^{-\bullet}{-}X \qquad (7)$$

$$\text{oxidation} \quad X{-}Q{-}X - 2e^- \rightarrow {}^{+\bullet}X{-}Q{-}X^{+\bullet} \qquad (8)$$

The separation between the forward and reverse peaks (ΔE_p) for oxidation of **MAPQ** is larger than the 59 mV expected for a nernstian reaction with no interaction between the groups[15] (e.g., $\Delta E_p = 70$ mV at $\nu = 100$ mV/s). While this might be taken to indicate a small interaction, we believe it is caused by uncompensated resistance, R_u, since the ΔE_p for reduction was 85 mV at $\nu = 100$ mV/s. We found R_u for benzene/MeCN (1:2) solution was about 1.7 kΩ, which could account for increases in the measured ΔE_p of about 10−20 mV at the peak currents found. To test the effect of R_u, we also examined the CV of ferrocene, which is a well-known nernstian, one electron oxidation wave at the scan rates used (100 mV/s to 10 V/s) under the same experimental conditions, and it showed the same increase in peak splitting.

Modified neglect of differential overlap (MNDO) semiempirical calculations were used to obtain an optimized molecular geometry of this compound to gauge the extent of charge localization upon the oxidation of **MAPQ**. These calculations show that the triphenylamine groups are twisted 58° from the plane of the central quinoxaline, indicating a lack of electron delocalization among these groups (Supporting Information, Figure S2), consistent with the electrochemical oxidative behavior of **MAPQ**.

The compounds **CFPP**, **CFPQ**, and **MFPQ** all contain pendent fluorene donor groups, rather than the triphenlyamines, on the quinoxaline. All exhibit reversible reduction waves in Bz: MeCN at $E_{1/2} = -0.9$, -0.82, and -1.46 V vs SCE, respectively. The electron withdrawing cyano groups on Q make **CFPP** and **CFPQ** much easier to reduce compared to **MFPQ** and **MAPQ**. Oxidation waves were observed for **CFPQ**, **CFPP** and **MFPQ** at potentials 1.76, 1.83, and 1.90 V, respectively, each of the oxidation waves involves a two electron transfer, which can be attributed to the two fluorene moieties. As with triphenylamine, the fact that a single 2e wave is obtained suggests both oxidize at the same potential because of only a small amount of delocalization through the center Q group. However $\Delta E_p \sim 170$ mV for oxidation waves, while $\Delta E_p \sim 80$ mV for the reduction, the same as observed for ferrocene under the same conditions ($\Delta E_p = 80$ mV). The larger ΔE_p for the oxidation, which is also larger than that of **MAPQ**, suggests some interaction (∼0.09 eV) between the groups in this case. The potentials for the oxidation are somewhat more positive than those seen with fluorenes or oligofluorenes with different substitution in earlier studies (∼1.2−1.4 V vs SCE).[3,16] On reversal following the anodic wave, a small wave was seen, in both **CFPQ** and **CFPP.** This could represent either the reduction of an impurity in the sample or from a small amount of product of a coupled chemical reaction of the oxidized form.

Digital simulations of cyclic voltammograms were undertaken to obtain preliminary information about possible mechanisms of the electrode reactions; more detailed studies are needed to obtain more definitive values of rate constants and mechanistic schemes. Figure 2 shows a comparison of the experimental and

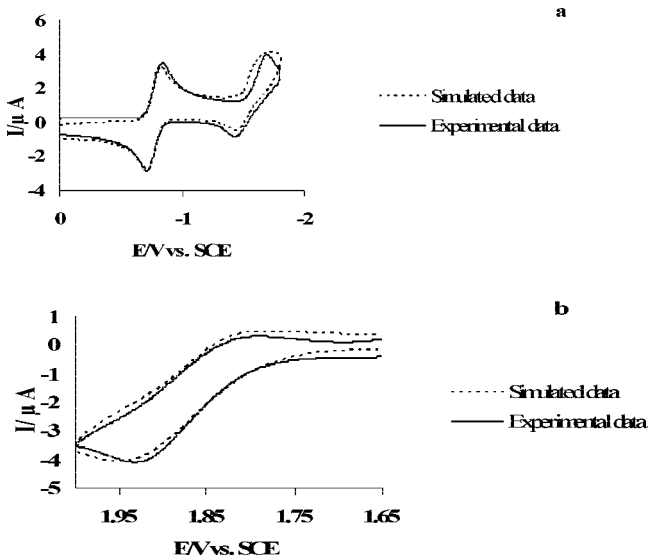

Figure 3. Comparison of the experimental and simulated data of 1 mM **CFPQ** ($v = 50$ mV/s). (a) The model for simulations of the two separated reduction steps was E, EC with $D = 3.4 \times 10^{-6}$ cm^2/s, $C_{dl} = 10$ μF/cm^2, $E^\circ_1 = -0.8$, $E^\circ_2 = -1.55$ V vs SCE, $k^\circ_1 \geq 0.1$ cm/s, $k^\circ_2 \geq 0.6$ cm/s and the homogeneous chemical reaction rate constant $k_f = 0.3$ s^{-1}. (b) The model of mechanism for oxidation of **CFPQ** was ECE with $k^o_1 \geq 0$. Two cm/s, $k^\circ_2 \geq 0.05$ cm/s and the homogeneous chemical reaction rate constant $k_f = 0.01$ s^{-1}.

simulated data of 1 mM **MAPQ** (at $v = 50$ mV/s) taking an uncompensated resistance, $R_u = 2$ kΩ. At this scan rate, there is a better fit if one adds a slow reaction of the radical anion following reduction of **MAPQ**, an EC mechanism. The best fit was with $n = 1$, heterogeneous electron transfer rate constant $k^\circ_1 \geq 0$. Two cm/s, $E^\circ = -1.40$ V and the following homogeneous chemical reaction rate constant $k_f = 0.07$ s^{-1}. For the oxidation of **MAPQ** the simulation shows an EE scheme, with $n_1 = n_2 = 1$, $D = 8.7 \times 10^{-6}$ cm^2/s, $E^\circ_1 = 1.2$, $E^\circ_2 = 1.25$ V vs SCE, $k^\circ_1 \geq 0.1$ cm/s, $k^\circ_2 \geq 0.6$ cm/s. Comparison of the experimental and simulated data of 1 mM **CFPQ** ($v = 50$ mV/s) is shown in Figure 3. The model of mechanism for oxidation of **CFPQ** was ECE, with $k^o_1 \geq 0$. Two cm/s, $k^\circ_2 \geq 0.05$ cm/s and the homogeneous chemical reaction rate constant $k_f = 0.01$ s^{-1}. The model for simulations of the two separated reduction steps was E, EC, $D = 3.4 \times 10^{-6}$ cm^2/s, $C_{dl} = 10$ μF/cm^2, $E^\circ_1 = -0.8$, $E^\circ_2 = -1.55$ V vs SCE, $k^\circ_1 \geq 0.1$ cm/s, $k^\circ_2 \geq 0.6$ cm/s and the homogeneous chemical reaction rate constant $k_f = 0.3$ s^{-1}.

Spectroscopy. The absorbance and fluorescence spectra of the compounds are shown in Figure 4, where the photoluminescence experiments were performed for all of the compounds in the same solvent mixture as that used for the electrochemical measurements. **MAPQ** shows a band with emission centered at 592 nm (excitation at 390 nm), while the emission of **MFPQ** when excited at 390 nm was considerably blue-shifted, with $\lambda_{max} = 448$ nm. This can be ascribed to the better donor ability of the triphenylamine group in **MAPQ** compared to that of the fluorenyl group in **MFPQ**, leading to an increase of HOMO level and for **MAPQ** compared with that of **MFPQ**, resulting in a smaller energy gap.

The Stokes shift in **MFPQ**, 40 nm, is much smaller than that of the other compounds: **MAPQ** (140 nm), **CFPP** (153 nm), and **CFPQ** (185 nm). **MFPQ** should show the smallest amount of D−A interaction among this group, and hence the smallest dipole moment. The smaller Stokes shift for **MFPQ** could then be attributed to the weaker interaction of both the ground and excited-state with the solvent.

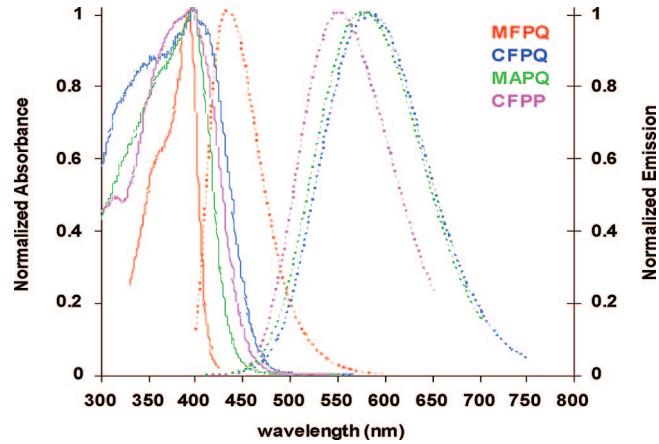

Figure 4. Absorbance spectra (solid lines) and fluorescence spectra (dotted lines), **MAPQ**, **CFPQ**, **CFPP**, and **MFPQ** (excitation wavelength, 390 nm), in benzene/acetonitrile (1:1) with 0.1 M $TBAPF_6$.

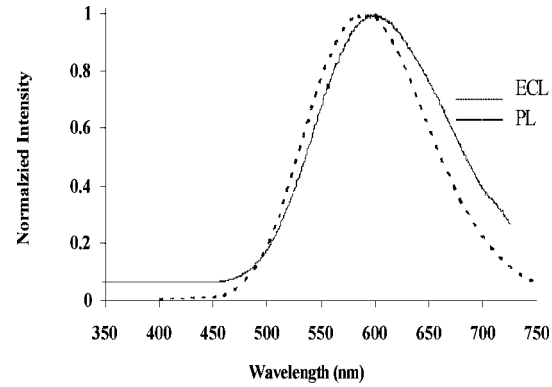

Figure 5. ECL (solid line) and PL (dashed line) spectra for **MAPQ** in MeCN, 0.1 M TBAP. PL (50 μM, 400−770 nm), ECL (0.5 mM, 1 mm slit, integration time, 2 min).

Electrogenerated Chemiluminescence. ECL was observed for all of the compounds by either potential steps or sweeps. With **MFPQ** the emission was too weak to obtain an ECL spectrum with the CCD, but we were able to detect ECL by pulsing the electrode with a 0.1 s pulse width and recording the total emission with the photomultiplier. Relatively strong ECL of **MAPQ** was observed in the same solvent as used in CV by alternately pulsing the electrode potential between 50 mV more negative than the first reduction peak potential ($E_{p,red}$) and 50 mV more positive than the first oxidation peak potential ($E_{p,ox}$). A comparison of the ECL and PL spectra of **MAPQ** is shown in Figure 5. The ECL spectrum showed a maximum at a wavelength around 600 nm, which was slightly red-shifted from PL spectrum. This difference between ECL and PL is frequently noticed and is probably due to an inner filter effect as a result of the higher concentrations of **MAPQ** needed to obtain measurable ECL.[17] The larger width in the ECL spectrum can be ascribed to the difference in resolution between the two instruments used to collect the spectra, since wider slits were needed in the ECL measurement. When pulsed at a potential slightly more positive than the first oxidation peak potential of the compound, a larger ECL signal was observed. Annihilation ECL of 1.0 mM **CFPQ** under the same conditions as the CV compared to the PL spectrum is shown in Figure 6. The ECL spectrum showed a maximum at wavelength ~605 nm, again slightly red-shifted from the PL spectrum (596 nm). ECL was obtained by continuous pulsing (pulse width 0.1 s) between the first oxidation peak and the first reduction peak in the same solutions as those used in the electrochemical studies, with mM

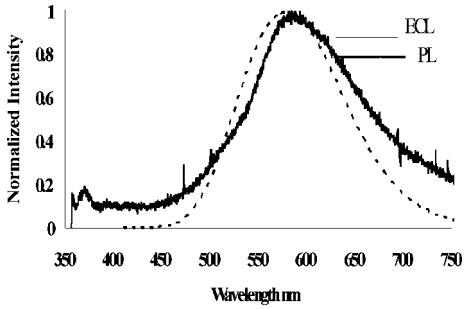

Figure 6. ECL (solid line) and PL (dashed line) spectra for **CFPQ** in benzene:MeCN (1:1), $TBAPF_6$ 0.1 M. PL (50 μM, 400−770 nm), ECL (0.5 mM, 1 mm slit, integration time 2 min).

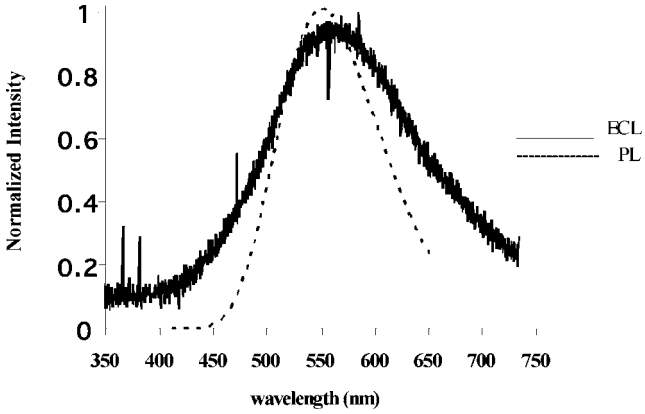

Figure 7. ECL and PL spectra for **CFPP** in benzene:MeCN (1:1), $TBAPF_6$ 0.1 M. PL (50 μM, 400−770 nm), ECL (0.5 mM, 1 mm slit, integration time 2 min).

levels of **CFPP** produced ECL emission that was readily observed with the naked eye in a slightly darkened room (Figure 7). As mentioned above an ECL spectrum for **MFPQ** was not obtained with the CCD; ECL detected with the PMT is shown in Supporting Information Figure S8.

The ECL annihilation reaction with these compounds is more complex than the case of simpler single charged monoanions and monocations. In this case the oxidized form is a dication; however, as it diffuses from the electrode surface, it encounters parent compound diffusing toward the electrode and thus undergoes a comproportionation reaction to produce cation radicals.

$$X-Q-X + {}^{+\bullet}X-Q-X^{+\bullet} \rightleftharpoons 2X-Q-X^{+\bullet} \qquad (9)$$

The equilibrium constant of this reaction is of the order of unity. Thus the ECL reaction could involve reaction of $X-Q^{-\bullet}-X$ with either ${}^{+\bullet}X-Q-X^{+\bullet}$ or $X-Q-X^{+\bullet}$. The energy available (enthalpy of annihilation, ΔH_{ann}) for these reactions, as calculated from the electrochemical data (shown in Table 1) is greater than the singlet energy, E_s, from the emission spectra, which assigns the ECL as an S-type (or energy sufficient) system.

Conclusions

The electrochemistry of a series of donor−acceptor compounds based on electron-accepting quinoxaline groups with two strong substituent donor groups based on triphenylamine or fluorene groups was investigated. The reduction produces the quinoxaline-centered anion radical and the oxidation at dication with charge centered on the very weakly interacting substituents. The annihilation reaction of the electrogenerated reduced and oxidized forms produces relatively strong ECL.

Semiempirical MNDO calculations of **MAPQ** show that the triphenylamine groups are twisted 58° from the plane of central quinoxaline, indicating a lack of electron delocalization between these groups. As a result of this slight interaction between the two triphenylamine groups, the oxidation of the first triphenylamine group creates a slight energetic barrier to the oxidation of the adjacent triphenylamine group, characterized by two closely spaced one-electron oxidation waves. Most importantly, the energy of the annihilation reaction for **MAPQ** and **CFPQ** is sufficient enough to generate the singlet-excited-state and corresponding ECL emission. Donor−acceptor ability such as this may provide a general approach to designing new materials exhibiting efficient ECL.

TABLE 1: Physical Data of the Ion Annihilation Reaction for ECL Data of Compounds[a]

compound	E_{red},V vs SCE[b]	E_{ox},V vs SCE[b]	D, 10^{-6} cm^2/s	$-\Delta G_{ann}$ (eV)[c]	$-\Delta H_{ann}$ (eV)[d]	E_S (eV)[e]
MAPQ	−1.72	1.26	8.6	2.98	2.88	2.1
CFPQ	−0.82	1.76	3.4	2.58	2.48	2.1
MFPQ	−1.46	1.87	2.8	3.33	3.23	2.8
CFPP	−0.9	1.83	3.2	2.73	2.63	2.3

[a] These experiments were performed for MAPQ at a 0.5 mm Pt disk electrode in Bz/MeCN 1:1 with 0.1 M TBAP as the supporting electrolyte, and in Bz/MeCN 1:1 with 0.1 M $TBAH_6$ for CFPQ, MFPQ and CFPP. [b] $E_{1/2} = (E_{pc} + E_{pa})/2$, except where otherwise specified. Peak potential of prewave. [c] $-\Delta G_{ann} = E_{pa}^{ox} - E_{pc}^{red}$. [d] $-\Delta H_{ann} = -\Delta G_{ann} - 0.1$.[18] [e] $E_s = 1239.85/\lambda_{max}^{PL}$ (nm).

Acknowledgment. The authors thank BioVeris Inc., the Robert A. Welch Foundation (F-0021), the National Science Foundation (CHE-0451494), and the National Natural Science Foundation of China (60736004, 50673093) for supporting this work. We appreciate helpful comments and suggestions by Dr. Fu-Ren F. Fan, and A.I. thanks the Shiraz University of Iran for granting leave for this study.

Supporting Information Available: Additional CVs, comparison experimental, simulated data and views of **MAPQ** with optimized ground-state molecular geometry as calculated by MNDO semiempirical calculations. This material is available free of charge via the Internet at http://pubs.acs.org.

References and Notes

(1) Chen, S. Y.; Xu, X. J.; Liu, Y. Q.; Qiu, W. F.; Yu, G.; Wang, H. P.; Zhu, D. B. *J. Phys. Chem.* **2007**, *111*, 1029–1034.

(2) (a) Palácios, R. E.; Fan, F.-R. F.; Barbara, P. F.; Bard, A. J. *J. Am. Chem. Soc.* **2006**, *128*, 9028–9029. (b) Goes, M.; Hoebe, N.; van Ramesdonk, H. J.; Verhoeven, J. W.; Werts, M. H. V.; Hofstraat, J. W.; Bakker, B. H. *Coord. Chem. Rev.* **2000**, *208*, 3. (c) Kulkarni, A. P.; Wu, P.-T.; Kwon, T. W.; Jenekhe, S. A. *J. Phys. Chem. B* **2005**, *109*, 19584.

(3) Fungo, F.; Wong, K.-T.; Ku, S.-Y.; Hung, Y.-Y.; Bard, A. J. *J. Phys. Chem. B* **2005**, *109*, 3984.

(4) (a) Facchetti, A.; Mushrush, M.; Yoon, M.-H.; Hutchison, G. R.; Ratner, M. A.; Marks, T. J. *J. Am. Chem. Soc.* **2004**, *126*, 13859. (b) Facchetti, A.; Letizia, J.; Yoon, M.-H.; Mushrush, M.; Katz, H. E.; Marks, T. J. *Chem. Mater.* **2004**, *16*, 4715.

(5) (a) Zhang, T.-G.; Zhao, Y.; Asselberghs, I.; Persoons, A.; Clays, K.; Therien, M. J. *J. Am. Chem. Soc.* **2005**, *127*, 9710. (b) Koynov, K.; Bahtiar, A.; Bubeck, C.; Mühling, B.; Meier, H. *J. Phys. Chem. B* **2005**, *109*, 10184. (c) Zhan, X.; Liu, Y.; Zhu, D.; Huang, W.; Gong, Q. *Chem. Mater.* **2001**, *13*, 1540. (d) Cai, C.; Liakatas, I.; Wong, M.-S.; Bösch, M.; Bosshard, C.; Günter, P.; Concilio, S.; Tirelli, N.; Suter, U. W. *Org. Lett.* **1999**, *1*, 1847.

(6) (a) Sun, X. B.; Liu, Y. Q.; Xu, X. J.; Yang, C. H.; Yu, G.; Chen, S. Y.; Zhao, Z. H.; Qiu, W. F.; Li, Y. F.; Zhu, D. B. *J. Phys. Chem. B* **2005**, *109*, 10786. (b) Wong, M. S.; Li, Z. H.; Tao, Y.; D'Iorio, M. *Chem.*

Mater. **2003**, *15*, 1198. (c) Jenekhe, S. A.; Lu, L.; Alam, M. M. *Macromolecules* **2001**, *34*, 7315.

(7) (a) Lai, R. Y.; Kong, X.; Jenekhe, S. A.; Bard, A. J. *J. Am. Chem. Soc.* **2003**, *125*, 12631–12639.

(8) (a) Richter, M. M.; Fan, F.-R. F.; Klavetter, F.; Heeger, A. J.; Bard, A. J. *Chem. Phys. Lett.* **1994**, *226*, 115. (b) Prieto, I.; Teetsov, J.; Fox, M. A.; Vanden Bout, D. A.; Bard, A. J. *J. Phys. Chem. A* **2001**, *105*, 520. (c) Janakiraman, U.; Doblhofer, K.; Fischmeister, C.; Holmes, A. B. *J. Phys. Chem. B* **2004**, *108*, 368. (d) Kulkarni, A. P.; Kong, X.; Jenekhe, S. A. *Adv. Funct. Mater.* **2006**, *16*, 1057–1066.

(9) (a) For review of ECL, see: BardA. J.; Faulkner, L. R. In *Electroanalytical Chemistry*; Bard, A. J., Ed.; Marcel Dekker: New York, 1977; Vol. 10, p 1. (b) Knight, A. W.; Greenway, G. M. *Analyst* **1994**, *119*, 879. (c) *Electrogenerated Chemiluminescence*; Bard, A. J., Ed.; Marcel Dekker: New York, 2004. (d) Knight, A. W.; Greenway, G. M. *Analyst.* **1995**, *120*, 1077.

(10) Miao, W. *Chem. Rev.* **2008**, *108*, 2506–2553.

(11) (a) Yu, J.; Fan, F.-R. F.; Pan, S.; Lynch, V. M.; Omer, K. M.; Bard, A. J. *J. Am. Chem. Soc.* **2008**, *130*, 7196–7197. (b) Chang, Y-L.; Palacios, R. E.; Fan, F-R. F.; Bard, A. J.; Barbara, P. F. *J. Am. Chem. Soc.* **2008**, *130*, 8906–8907.

(12) Debad, J.; Lee, S. K.; Qiao, X.; Pascal, R. A.; Bard, A. J. *Acta Chem. Scand.* **1998**, *52*, 45.

(13) Fabrizio, E. F.; Payne, A.; Westlund, N. E.; Magnus, P. P.; Bard, A. J. *J. Phys. Chem.* **2002**, *106*, 1961.

(14) Debad, J. D.; Morris, J. C.; Magnus, P.; Bard, A. J. *J. Org. Chem.* **1997**, *62*, 530.

(15) Bard, A. J.; Faulkner, L. R. *Electrochemical Methods: Fundamentals and Applications*, 2nd ed.; John Wiley & Sons: New York, 2001; pp 234−238.

(16) Omer, K. M.; Kanibolotsky, A. L.; Skabara, P. J.; Perepichka, I. F.; Bard, A. J. *J. Phys. Chem. B* **2007**, *111*, 6612–6619.

(17) Ding, Z. F.; Quinn, B. M.; Haram, S. K.; Pell, L. E.; Korgel, B. A.; Bard, A. J. *Science* **2002**, *296*, 1293.

(18) Santa Cruz, T. D.; Akins, D. L.; Birke, R. L. *J. Am. Chem. Soc.* **1976**, *98*, 1677.

JP807202D